Bidirectional Transepithelial IgG Transport by a Strongly Polarized Basolateral Membrane Fcγ-Receptor □

Steven M. Claypool,*† Bonny L. Dickinson,‡ Jessica S. Wagner,‡ Finn-Eirik Johansen,‡ Nanda Venu,‡ Jason A. Borawski,‡ Wayne I. Lencer,‡¶# and Richard S. Blumberg†§¶#

Harvard Medical School, *Program in Immunology and Departments of §Medicine and †Gastroenterology Division, Brigham and Women's Hospital, Boston, Massachusetts 02115; and ‡Gastrointestinal Cell Biology and Department of Medicine, Children's Hospital, Boston Massachusetts 02115; and ¶the Harvard Digestive Diseases Center, Boston, Massachusetts 02115

The human MHC class I–related neonatal Fc receptor, hFcRn, mediates bidirectional transport of IgG across mucosal barriers. Here, we find that at steady state hFcRn distributes predominantly to an apical intracellular compartment and almost exclusively to the basolateral cell surface of polarized epithelial cells. It moves only transiently to the apical membrane. Ligand binding does not redistribute the steady state location of the receptor. Removal of the cytoplasmic tail that contains di-leucine and tryptophan-based endocytosis motifs or incubation at low temperature (18°C) redistributes the receptor apically. The rates of endocytosis of the full-length hFcRn from the apical or basolateral membrane domains, however, are equal. Thus, the strong cell surface polarity displayed by hFcRn results from dominant basolateral sorting by motifs in the cytoplasmic tail that nonetheless allows for a cycle of bidirectional transcytosis.

INTRODUCTION

The numerous studies on the cell biology of the polymeric immunoglobulin receptor (pIgR) and transferrin receptor (TfnR) as expressed in the Madin-Darby canine kidney (MDCK) cell line have provided a detailed characterization of the itineraries of these proteins undergoing such processes as basolateral recycling, basolateral to apical transcytosis, and apical recycling in MDCK cells (Mostov and Deitcher, 1986; Leung *et al.,* 1999; Brown *et al.,* 2000; Wang *et al.,* 2000). Comparatively little is known about trafficking in the apical to basolateral direction because of the lack of a model protein that physiologically harnesses this pathway, and whether the trafficking of pIgR and TfnR can be generalized to the trafficking of other proteins in polarized cells remains to be tested.

The MHC class I–related neonatal Fc receptor, FcRn, is responsible for the absorption of maternal IgG across the rabbit and rodent yolk sac, the human placenta, and the proximal small intestine of the neonatal rodent (Rodewald, 1970; Simister and Mostov, 1989; Roberts *et al.,* 1990; Medesan *et al.,* 1996; Firan *et al.,* 2001). Absorption of IgG depends on the ability of FcRn to bind IgG and traffic bidirectionally across the epithelial cells that line the lumen of these tissues (Jones and Waldmann, 1972; Abrahamson and Rodewald, 1981; Dickinson *et al.,* 1999; McCarthy *et al.,* 2000; Kobayashi *et al.,* 2002). Almost nothing is known about the cellular mechanisms that explain how any membrane receptor can move bidirectionally across polarized epithelial cells.

Like most other MHC class I–related molecules, FcRn is an obligate heterodimer consisting of a glycosylated heavy (α) chain (40–44 kDa in humans, 48–50 kDa in rodents) that associates noncovalently with β2-microglobulin (β_2m; Simister and Mostov, 1989). The association with β_2m is species dependent (Claypool *et al.,* 2002), and the functional receptor is likely a dimer of heterodimers that binds one IgG molecule (Burmeister *et al.,* 1994; Kim *et al.,* 1994). The Fc fragment of IgG binds to FcRn at acidic pH (pH ≤6.5) and releases from the receptor at neutral pH (Rodewald, 1976). In cells expressing FcRn, the bulk of FcRn is located intracellularly at steady state (Berryman and Rodewald, 1995; Dickinson *et al.,* 1999; Ober *et al.,* 2001). Ligand binding to FcRn can occur either at the cell surface or in the acidic endosome (Dickinson *et al.,* 1999; Wu and Simister, 2001; Kobayashi *et al.,* 2002). Trafficking of the rat FcRn in polarized cells depends on sorting motifs in the cytoplasmic tail (Stefaner *et al.,* 1999; McCarthy *et al.,* 2001; Wu and Simister, 2001). Mutation of a di-leucine motif and a tryptophan residue in the cytoplasmic tail of rat FcRn impairs endocytosis of the receptor from both apical and basolateral membrane

domains, with a more severe reduction in endocytosis observed from the apical surface. Removal of the entire cytoplasmic tail strongly inhibits basolaterally directed IgG transport but has no detectable effect on the apically directed transport pathway (Wu and Simister, 2001). There are conflicting results, however, on whether the FcRn cytoplasmic tail affects sorting in the biosynthetic pathway (Stefaner *et al.*, 1999; Wu and Simister, 2001).

In mammals that absorb IgG from breast milk, expression of FcRn in the intestine is strongly downregulated after weaning (Brambell, 1966; Simister and Mostov, 1989). In humans and nonhuman primates, the intestine continues to express FcRn into adult life (Dickinson *et al.*, 1999; Zhu *et al.*, 2001). FcRn is also expressed in the epithelium lining the lung in adult mice, humans, and nonhuman primates (Spiekermann *et al.*, 2002). At these sites, FcRn mediates IgG transport across the mucosal barrier and may function in immune surveillance and host defense. In all species studied so far, FcRn has also been shown to extend IgG half-life by binding IgG in endosomes of endothelial cells (Borvak *et al.*, 1998; Ward *et al.*, 2003) and recycling the bound IgG back out of the cell, away from the late endosome and lysosome where degradation of unbound IgG occurs.

Nothing is known about how hFcRn operates in a polarized cell except that it is capable of mediating the bidirectional transport of IgG via a transcytotic mechanism that requires endosomal acidification (Dickinson *et al.*, 1999; Claypool *et al.*, 2002; Kobayashi *et al.*, 2002). Previous studies on hFcRn in MDCK cells are not conclusive because the human heavy chain was expressed in cells lacking human β_2m (Praetor *et al.*, 1999). Chimeras of the human FcRn heavy chain and canine β_2m do not traffic normally (Claypool *et al.*, 2002).

Here, we study the trafficking of hFcRn in polarized epithelial cells by heterologous expression of the hFcRn heavy chain in a hβ_2m-positive MDCK cell line. We find that trafficking of human FcRn differs from that of the rat FcRn (Stefaner *et al.*, 1999; McCarthy *et al.*, 2000; McCarthy *et al.*, 2001; Wu and Simister, 2001) and from previous claims on the human receptor (Praetor *et al.*, 1999). Like the rat receptor, human FcRn predominantly localizes to a supra-nuclear intracellular compartment and mediates bidirectional transcytosis of IgG, but unlike the rat receptor, the fraction of human FcRn on the cell surface at steady state is almost exclusively basolateral and the efficiency of transport is strongly apically directed. Although ligand binding does not affect the distribution of hFcRn, either removal of the cytoplasmic tail or incubation at low temperature (18°C) redistributes the receptor apically, and the fact that the rates of endocytosis of the full-length receptor from the apical and basolateral membranes are equal suggests that the steady state distribution of hFcRn is maintained by a dominant basolateral sorting signal(s) contained in the tail domain that is functionally temperature sensitive. Unlike other rapidly recycling receptors that sort strongly to the basolateral membrane by motifs contained in the cytoplasmic tail, however, the bidirectional trafficking by FcRn through the transcytotic pathway is not stochastic and occurs at physiological rates.

MATERIALS AND METHODS

Plasmid Construction and Recombinant Protein Expression

The hβ_2m and hFcRn expression vectors have been described previously (Claypool *et al.*, 2002). Generation of a tailless hFcRn containing an NH$_2$-terminal hemaglutinin (HA) tag (5′-YPYDVPDYA-3′) was performed as described (Claypool *et al.*, 2002) by introducing a stop translation site immediately after the first four predicted amino acids of the hFcRn cytoplasmic tail (RRMR; Story *et al.*, 1994). All constructs described were verified by sequencing.

To generate recombinant human IgG1 with specificity for the hapten 5-iodo-4-hydroxy-3-nitro-phenylacetyl (NIP), pLNOH2-IgG1 (gift from T.E. Michalesen, Norwegian Institute of Public Health) containing an exon encoding a NIP-specific variable domain spliced to a downstream human IgG1 heavy-chain constant region (Norderhaug *et al.*, 1997) was transfected into the murine myeloma cell line J558L, and clonal lines selected. J558L cells express endogenous λ light chain that can combine with the chimeric heavy chain to form NIP-specific antibody with the human IgG1 Fc region (NIP-hIgG1). NIP-hIgG1 affinity purification was performed as described (Johansen *et al.*, 1999).

Antibodies

The mouse monoclonal antibodies (mAbs) 12CA5, reactive against the influenza HA epitope, and BBM1, specific for hβ_2m, and the rabbit anti-hFcRn cytoplasmic tail domain polyclonal antiserum have been described (Claypool *et al.*, 2002). The guinea pig anti-hFcRn cytoplasmic tail domain antiserum was a kind gift of Syntonix Pharmaceuticals (Waltham, MA). Pooled human IgG was obtained from Lampire Biological Laboratories (Pipersville, PA) and Chicken IgY from Gallus Immunotech Inc. (Wildwood, MO). Other antibodies used were: rabbit anti-hβ_2m and anti-HA polyclonal antisera, mouse anti–β-actin and anti–ZO-1 mAbs (Sigma Chemical Co., St. Louis, MO), chicken anti-human IgG Alexa 488 (Molecular Probes, Eugene, OR), mouse anti-transferrin receptor (Zymed, South San Francisco, CA), mouse anti–E-cadherin mAb (clone E4.6, kind gift of Drs. John Higgins and Michael Brenner; Cepek *et al.*, 1994), mouse anti-GP135 mAb (Ojakian and Schwimmer, 1988), and rabbit antiserum reactive to human CD55 (Santa Cruz Biotechnology, Santa Cruz, CA). Alexa-conjugated, horseradish peroxidase (HRP)-conjugated, and alkaline phosphatase–conjugated IgG were from Molecular Probes, Pierce (Rockford, IL) and Sigma, respectively.

Cell Culture

Stable MDCK cell transfectants were prepared and cultured as previously described (Claypool *et al.*, 2002). A stable hβ_2m-positive parental MDCK clone was supertransfected with either full-length HA-tagged hFcRn or tailless HA-tagged hFcRn plasmids. MDCK II cells transfected with the parental pcDNA3.1 and pEF6/V5-HisA vectors (Invitrogen, Carlsbad, CA) were generated as negative controls.

T84 cells were passaged weekly and maintained in a 1:1 mixture of low-glucose DMEM and F-12 Nutrient Mixture containing 0.014 M NaHCO$_3$, 0.015 M HEPES, pH 7.3, and 6% heat-inactivated FBS at 37°C, 5% CO$_2$. Caco-2 cells were passaged weekly and maintained in high-glucose DMEM containing 10% FBS and 15 mM HEPES, pH 7.4, at 37°C, 5% CO$_2$. For the selective cell surface biotinylation studies, T84 and Caco-2 cells were seeded at confluent density onto 24-mm, 3-μm pore size, semipermeable polycarbonate Transwell filters (Corning Inc., Corning, NY) that were collagen coated (mouse collagen Type IV; BD Biosciences, Bedford, MA) 24 h earlier. Transepithelial resistances were recorded daily for each filter, medium was replenished every 2–3 days, and experiments were performed 11–15 days postplating at which point the resistances measured ≥1000 and 250–300 Ωcm^2 for T84 and Caco-2 monolayers, respectively.

MDCK clones were plated at confluent density on 24-mm diameter, 0.4-μm pore size, semipermeable polycarbonate Transwell filters or on 6.5-mm diameter, 0.4-μm pore size, optically clear semipermeable polyester Transwell filters for biochemical studies and immunofluorescence experiments, respectively. Experiments were performed day 3 or 4 postplating. For serum starvation, filters were incubated for 1 h in serum-free medium buffered to pH 7.3 with 20 mM HEPES. To assess the effect of ligand with or without a pH gradient on the steady state distribution of hFcRn, human IgG or chicken IgY (100 μg/ml) was added to DMEM containing 2% FBS buffered to either pH 7.3 with 20 mM HEPES or buffered to pH 6.0 with 20 mM MES. Ligand was added to the input chamber. DMEM containing 2% FBS, 20 mM HEPES, pH 7.3, was added to the output chamber, and the filters incubated for 12 h at 37°C, 5% CO$_2$ before domain selective biotinylation. For colocalization, after a 1-h serum starvation, DMEM containing 0.2% BSA buffered at pH 7.3 or 6.0 and supplemented with 100 μg/ml human IgG1/κ (Sigma) was applied as indicated. IgG uptake was visualized after incubation at 37°C, 5% CO$_2$ for 20 min. All 18°C incubations were performed for the indicated times utilizing a cooled H$_2$O bath.

IgG Binding

Cell lysates were prepared as described (Claypool *et al.*, 2002). Defined quantities of lysate (Figure 1 caption) were incubated for 4 h with 200 μg human IgG, rotating gently at 4°C, and were captured on protein G-Sepharose beads (Amersham Biosciences, Piscataway, NJ). After three successive washes with 1 mg/ml CHAPS, pH 6.0 or 8.0, bound proteins were resolved on 12% SDS-PAGE gels under nonreducing conditions. All immunoblot analyses, including stripping and reprobing of nitrocellulose membranes (Schleicher & Schuell, Keene, NH) and densitometric analyses of films were performed as previously described (Claypool *et al.*, 2002).
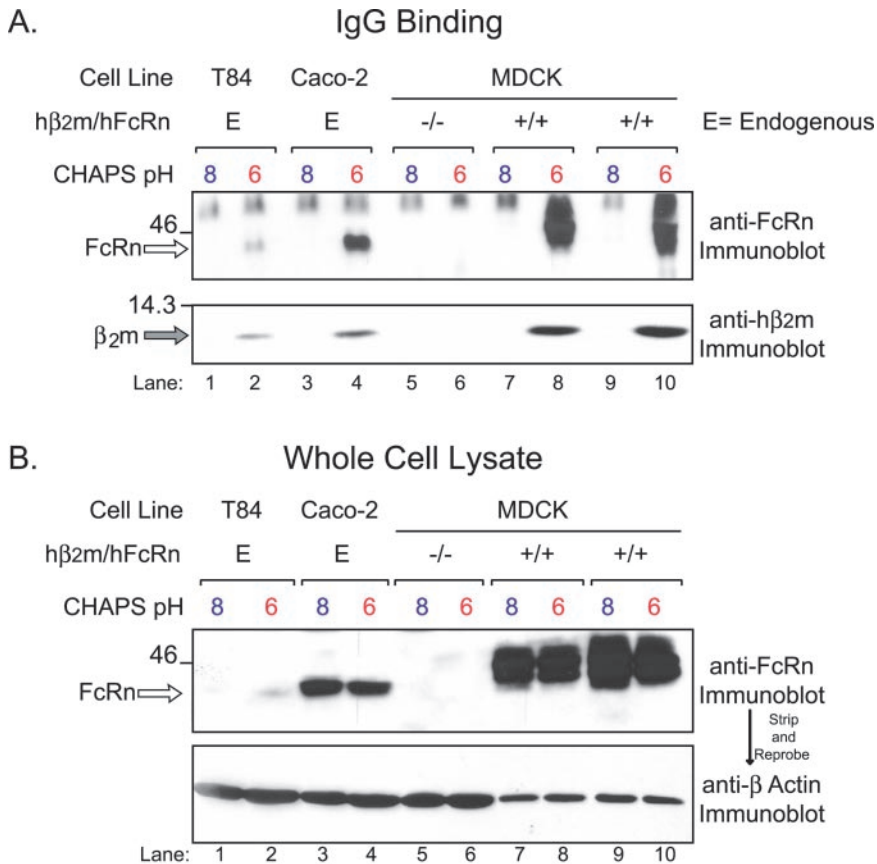
A. **IgG Binding**

B. **Whole Cell Lysate**

Figure 1. Both endogenous and transfected hFcRn bind human IgG with strict pH dependency. (A) Human IgG was preincubated with cell lysates prepared in CHAPS lysis buffer, pH 6.0 or 8.0, and subsequently captured by the addition of protein G-Sepharose. Bound proteins were analyzed by SDS-PAGE under nonreducing conditions and immunoblotted for hFcRn (top) and hβ_2m (bottom). The following cell lines were examined for IgG binding with the quantity of lysate indicated in parentheses: T84 cells (1 mg), Caco-2 (1 mg), a control hβ_2m−/hFcRn− MDCK clone (1 mg), and two hβ_2m+/hFcRn+ MDCK clones (0.2 mg). (B) Total hFcRn was immunoblotted in each of the following lysates: T84 (50 μg), Caco-2 (50 μg), a control hβ_2m−/hFcRn− MDCK clone (50 μg), and two individual hβ_2m+/hFcRn+ MDCK clones (10 μg). The bottom panel is the same membrane reprobed for β-actin. The location of bands consistent with the predicted sizes of hFcRn (open arrow) and hβ_2m (gray arrow) are indicated on the left of each gel. Size markers (kDa) are indicated on the left.

Transcytosis Assay and ELISA

Transcytosis assays were performed as described (Claypool *et al.,* 2002) with the following modifications. Monolayers were washed with Hanks' balanced salt solution at pH 7.4 with 10 mM HEPES (HBSS+, pH 7.4), followed by a 20-min incubation at 37°C, 5% CO$_2$ with either 1% BSA in HBSS+, pH 6.0 (HBSS+ buffered with 10 mM MES) or 1% BSA in HBSS+, pH 7.4, on the input surface and HBSS+, pH 7.4, on the opposite, output surface. NIP-hIgG1 was added to the input surface (60 nM final concentration), and the cells were maintained for 90 min at 37°C, 5% CO$_2$. For blocking experiments, rabbit IgG was included in the buffer applied to the input surface 20 min before the addition of NIP-hIgG1. After the 90-min incubation, the entire output solution was collected and transferred to a 96-well plate previously coated with BSA-NIP and blocked with BSA. Bound NIP-hIgG1 was detected by a human IgG-specific ELISA, and data were analyzed using SigmaStat 1.0 Software (Jandel Corporation, San Rafael, CA).

Immunocytochemistry and Confocal Microscopy

Immunocytochemistry of MDCK cells grown on Transwell inserts was performed as described (Claypool *et al.,* 2002). All images were collected using a 60×/1.4 NA oil immersion objective and Nikon Axiophot (Garden City, NY) coupled to a MRC1024 laser scanning confocal system (Bio-Rad Laboratories, Hercules, CA). All images were gathered using the same laser power, gain, and pinhole size for the respective channels. For each insert analyzed, two or more separate fields of cells were imaged (92 ìm^2 each, later cropped to 34 ìm^2). Serial *x-y* scans were collected using ZO-1 as a reference point. Final image processing and labeling were performed using Adobe Photoshop (Mountain View, CA).

Cell Surface Biotinylation

Domain selective biotinylation of filter-grown cells was performed as described (Casanova *et al.,* 1991). Cell lysis and immunoprecipitation of either full-length hFcRn or hFcRntl− was performed as described (Claypool *et al.,* 2002) using a rabbit anti-hFcRn cytoplasmic tail antiserum and 12CA5, respectively. For T84 and Caco-2 cells, the immunoprecipitates were analyzed directly by SDS-PAGE, and surface hFcRn was detected by immunoblotting with HRP-conjugated neutravidin (Pierce, 1:10,000). For the MDCK clones, immunoprecipitated proteins were eluted by boiling for 10 min in 24 μL 10% SDS. Ten percent of the eluate was set aside for direct analysis, and the

remaining 90% was diluted in 1 ml reprecipitation buffer (50 mM Tris, pH 7.4, 150 mM NaCl, 1% NP-40, 0.5% sodium deoxycholate, 0.2% BSA), and surface proteins were captured with avidin-agarose (Pierce). In every experiment, total surface proteins were captured either from a separate portion of the original biotinylated lysate or from the nonbinding flow through fraction after FcRn immunoprecipitation, by the addition of avidin-agarose.

Antibody Capture

Monolayers were serum-starved and equilibrated in DMEM, 0.2% BSA, pH 7.3, at the indicated temperatures for 20 min before the addition of 10 μl 12CA5 ascites to either the apical or basolateral chambers. After 90-min incubations, unbound antibody was removed by four successive 10-min washes with PBS, 0.1 mM CaCl$_2$, 1 mM MgCl$_2$, and 1% BSA at 4°C. Equal volumes of cell lysates (described above) were added directly to protein A-Sepharose and rotated at 4°C for 90 min. Twenty microliters of each sample was used for a β-actin immunoblot analysis.

Endocytosis Assay

Endocytosis of hFcRn was assayed as described (Graeve *et al.,* 1989). Equal quantities of lysate were added to avidin-agarose to capture total biotinylated surface proteins. Two filters were maintained at 4°C throughout the entire experiment, one serving as the biotinylation control (no reduction, time 0 min) and the other serving as a control for the reduction step. After extensive washing, the samples were resolved under reducing conditions on 10% SDS-PAGE gels, and immunoblot analyses were performed as described (Claypool *et al.,* 2002). Twenty microliters of each sample was collected for β-actin immunoblot analysis.

RESULTS

Functional Expression of hFcRn in MDCK Cells

To study trafficking of hFcRn in polarized epithelia, we prepared a stable MDCK cell line expressing hβ_2m and then supertransfected this cell line with a plasmid encoding the full-length hFcRn heavy chain containing an N-terminal HA tag. To demonstrate FcRn function, we first assessed the

pH-dependent binding of IgG to FcRn (Figure 1). The human intestinal epithelial cell lines, T84 and Caco-2, which express endogenous hFcRn, served as positive controls. MDCK cells transfected with empty vectors provided negative controls. Equal quantities of cell lysates were buffered at pH 6.0 or 8.0 and incubated with human IgG. IgG-binding proteins were then captured by incubation with protein G-Sepharose and analyzed for hFcRn and hβ_2m by SDS-PAGE and immunoblot. At acidic pH, IgG coprecipitated with both hFcRn (Figure 1A, top panel) and hβ_2m (Figure 1A, bottom panel, lanes 2, 4, 8, and 10). There was no FcRn isolated by IgG added to lysates of MDCK cells transfected with vector alone (lanes 5 and 6) or from any cell lysate buffered at pH 8.0 (lanes 1, 3, 7, and 9). FcRn was, however, present in the total cell lysates from all cells transfected with FcRn, whether buffered at pH 6.0 or 8.0 (Figure 1B, top panel). The migration of the HA-tagged hFcRn heavy chain in MDCK cells was slightly delayed compared with endogenous hFcRn in T84 and Caco-2 cells, consistent with the addition of the HA-tag, and the protein bands appeared more heterogeneous, consistent with the differential patterns of glycosylation observed in proteins heterologously expressed in MDCK cells (Singer and Mostov, 1998). Immunoblot for β-actin shows that each lane was loaded with an equal mass of total cell protein (Figure 1B, bottom panel). These data show that the hFcRn/hβ_2m heterodimer expressed in canine MDCK cells can bind human IgG at acidic but not basic pH, a hallmark of FcRn function.

To test for FcRn-mediated transcytosis, we used a recombinantly expressed and purified chimeric mouse/human IgG1 antibody reactive to the haptene 5-iodo-4-hydroxy-3-nitro-phenylacetyl (NIP-hIgG1, see MATERIALS AND METHODS). When tested in vitro, the recombinant NIP-hIgG1 antibody coprecipitated with hFcRn and hβ_2m in detergent lysates of MDCK cells at pH 6.0 but not at pH 8.0 (our unpublished results). FcRn-mediated transcytosis of NIP-hIgG1 was measured by ELISA for transport in both the apical to basolateral and basolateral to apical directions (Figure 2, A and B, respectively). In some studies, the pH of the input reservoir was buffered to 6.0 to increase IgG uptake by FcRn (McCarthy et al., 2001). The output reservoir was always buffered at pH 7.4 to favor release of NIP-hIgG1 after transcytosis.

In the apical to basolateral direction, FcRn-mediated transport of NIP-hIgG1 was observed for FcRn-expressing cell lines when the input reservoir was buffered at pH 6.0. Small amounts of Nip-hIgG1 were transported when the input reservoir was buffered to pH 7.4. Transport was specific for FcRn because it was not observed in cell lines that lacked hFcRn, and it was inhibited dose-dependently by competition with rabbit IgG that also binds hFcRn (Figure 2A). In the basolateral to apical direction (Figure 2B), receptor-mediated transport of NIP-hIgG1 was observed when the input reservoir was buffered at pH 7.4, but transcytosis of NIP-hIgG1 was 10-fold greater when the input reservoir was buffered to pH 6.0. Transport in this direction was also specific for hFcRn because no transport was observed in cell lines lacking hFcRn, and it was inhibited dose-dependently by competition with rabbit IgG. Consistent with our initial studies on FcRn in MDCK cells (Claypool et al., 2002), the mass of NIP-hIgG1 transported was greater in the basolateral to apical direction. Thus, hFcRn expressed in the hβ_2m-containing MDCK cell line functions in bidirectional IgG transport. These data are consistent with our previous findings that FcRn functions to transcytose IgG in both directions across polarized T84 cells expressing FcRn endogenously (Dickinson et al., 1999).
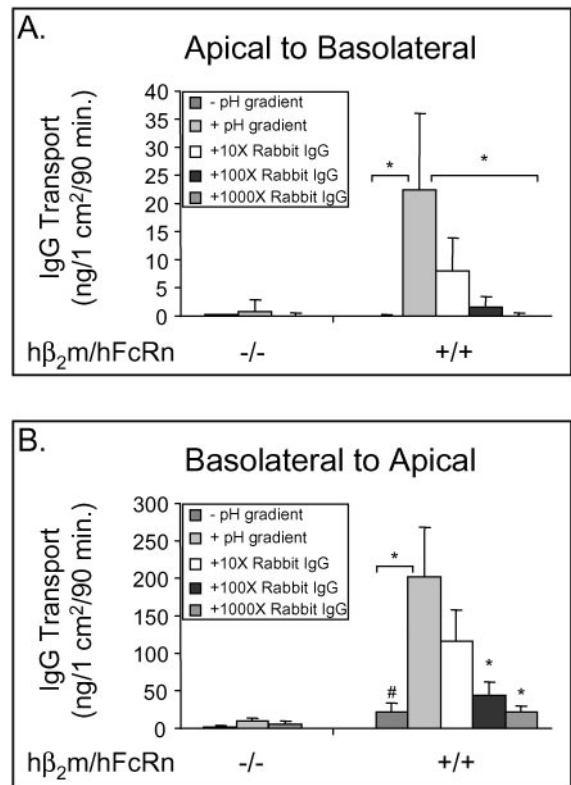

Figure 2. Bidirectional transcytosis of IgG by hFcRn expressed in hβ_2m-positive MDCK cells. Regardless of the direction, transcytosis assays were performed with the pH of the input chamber buffered at either pH 7.4 ($-$ pH gradient) or pH 6.0 ($+$ pH gradient), whereas the output chamber was always buffered at pH 7.4. For blocking experiments, the indicated concentration of rabbit IgG relative to NIP-hIgG1 was included in the input chamber that was buffered at pH 6.0. (A) Transcytosis of NIP-hIgG1 (60 nM final concentration) in the apical to basolateral direction. (B) Transcytosis of NIP-hIgG1 in the basolateral to apical direction. For ease of representation, data from two individual hβ_2m+/hFcRn+ clones were combined. ANOVA on Ranks, p $\leq$ 0.00001. The asterisk indicates statistical significance relative to NIP-hIgG1 transport with a pH gradient but in the absence of competitive ligand at p $\leq$ 0.05 by multiple comparison procedures. The number sign indicates statistical significance relative to transport of NIP-hIgG1 in the absence of a pH gradient by the hβ_2m$-$/hFcRn$-$ MDCK clone at p $\leq$ 0.05 by multiple comparison procedures (n = 3).

Human FcRn Localizes Predominantly to Intracellular Compartments and Colocalizes with Internalized IgG

We next analyzed the location of hFcRn in polarized MDCK cells expressing hFcRn by confocal microscopy. In the presence of IgG, the bulk of hFcRn localized to the apical region of the cell, beginning just below the level of the tight junction and extending ~4 μm down toward the basolateral plasma membrane (Figures 3 and 4, red). The same distribution was observed in the absence of added IgG (our unpublished results). Thus, ligand binding to FcRn does not redistribute the steady state localization of hFcRn in MDCK cells. The subapical distribution of hFcRn in MDCK cells is also consistent with the predominantly apical intracellular distribution of FcRn in human intestine and lung (Dickinson et al., 1999; Spiekermann et al., 2002) and rat intestine in vivo (Berryman and Rodewald, 1995).

IgG internalized for 20 min at pH 6.0 from the apical surface (Figure 3) or at pH 6.0 or 7.4 from the basolateral cell
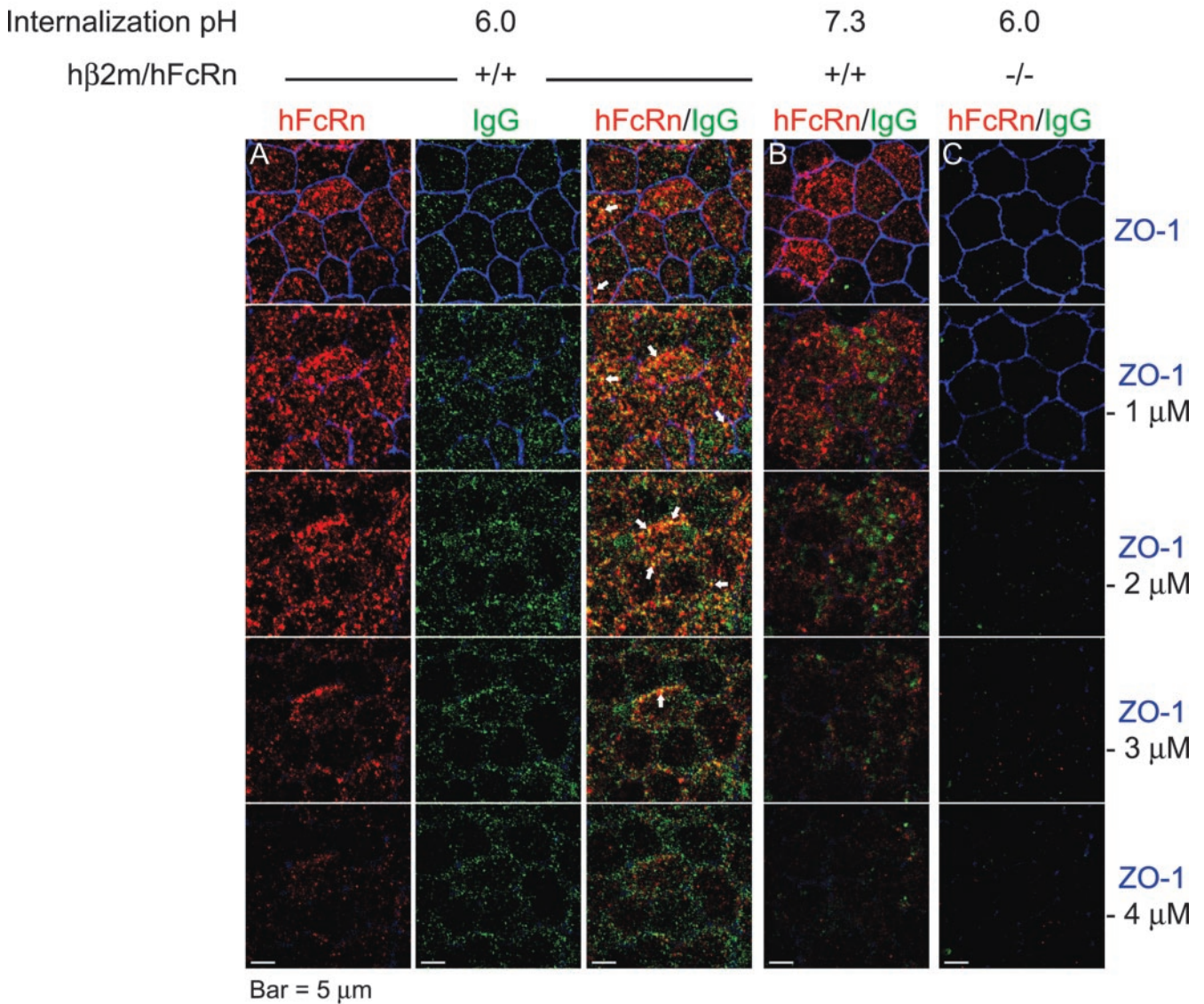
Apical Internalization

Figure 3. IgG internalization is enhanced from the apical plasma membrane and colocalizes with hFcRn when buffered at pH 6.0 but not at pH 7.3. After serum starvation, 625 nM human IgG1/*k* buffered at pH 6.0 (A and C) or pH 7.3 (B) was internalized from the apical chambers of filter-grown $h\beta_2m+$/hFcRn+ (A and B) and control (C) MDCK cells for 20 min at 37°C. The cells were fixed, and hFcRn (red), ZO-1 (blue), and human IgG (green) were detected using Alexa-conjugated secondary antibodies. Serial red, green, and blue images were separately collected utilizing a confocal microscope and merged images generated using Adobe Photoshop. (A) For internalization of IgG at pH 6.0 by $h\beta_2m+$/hFcRn+ MDCK cells, the position of hFcRn (red) and IgG (green) with respect to ZO-1 (blue) are presented individually (left two columns) and merged (right column). (B and C) For simplicity, only merged images are presented. The position of each merged *X-Y* plane relative to the tight junction (ZO-1) is indicated at the right. Arrows highlight regions of intense hFcRn and IgG colocalization (n = 3). Bars, 5 μm.

surface (Figure 4) colocalized with hFcRn. There was more IgG internalized at pH 6.0 than at pH 7.4, consistent with our functional studies (see Figure 2). Only very little IgG accumulated inside of MDCK cells lacking FcRn (Figure 3C and 4C, green). As expected for a transporting receptor, IgG colocalized with hFcRn at several planes of the cell, including the lateral aspects below the tight junction when loaded apically (Figure 3A, arrows in merged panels) and at the level of the tight junction when loaded basolaterally (Figure 4, A and B, arrows in merged panels). Taken together, the

biochemical, morphologic, and functional studies described above show that MDCK cells coexpressing $h\beta_2m$ and hFcRn heavy chain accurately model the biology of FcRn in polarized human epithelial cells in vitro and in vivo.

The Fraction of hFcRn on the Cell Surface Localizes Almost Exclusively to the Basolateral Plasma Membrane
We next analyzed the cell surface distribution of hFcRn (Figure 5). MDCK cells expressing the hFcRn heterodimer (lanes 4–9), $h\beta_2m$ alone (lanes 10–12), or not expressing
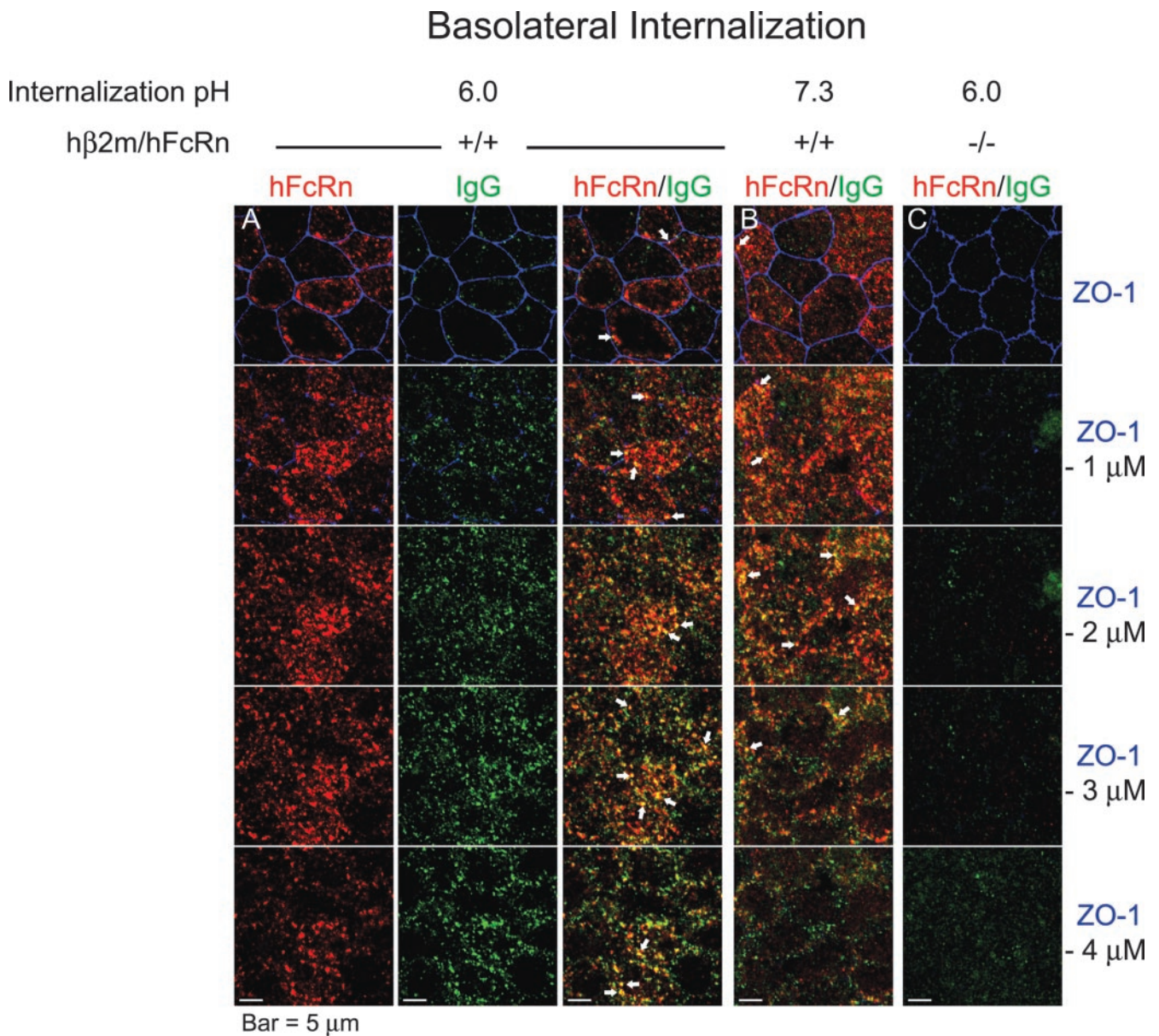
Basolateral Internalization

Figure 4. IgG is internalized from the basolateral plasma membrane and colocalizes with hFcRn when buffered at pH 6.0 and pH 7.3. Serum starvation and IgG internalization were performed as described in Figure 3 except that the IgG buffered at pH 6.0 (A and C) or pH 7.3 (B) was added to the basolateral compartment of filter-grown hβ_2m+/hFcRn+ (A and B) and control (C) MDCK cells. Detection of hFcRn (red), IgG (green), and ZO-1 (blue) and image collection and processing were performed as in Figure 3. (A) For internalization of IgG at pH 6.0 by hβ_2m+/hFcRn+ MDCK cells, the position of hFcRn (red) and IgG (green) with respect to ZO-1 (blue) are presented individually (left two columns) and merged (right column). (B and C) For simplicity, only merged images are presented. The position of each merged X-Y plane relative to the tight junction (ZO-1) is indicated at the right. Arrows highlight regions of intense hFcRn and IgG colocalization. Bars, 5 μm. (n = 3)

either chain (lanes 1–3) were treated at 4°C with sulfo-NHS-biotin applied selectively to apical or basolateral cell surfaces, or to both cell surfaces, to label apical or basolateral membrane proteins or proteins on both membranes. Some monolayers were serum starved for 1 h at pH 7.3 to dissociate bovine IgG from FcRn before domain-specific biotinylation (lanes 13–18). The monolayers were then lysed in detergent, and hFcRn was immunoprecipitated. Each immunoprecipitate was eluted by boiling in SDS, and 10% was set aside to assess total FcRn content. The remaining 90% was incubated with avidin-agarose beads to affinity-isolate bio-

tinylated cell surface-proteins. Both sets of samples were analyzed for HA-tagged FcRn by SDS-PAGE and immunoblotting for the hFcRn heavy chain (using an anti-HA mAb). All MDCK cells expressing hFcRn contained hFcRn in the immunoprecipitates (Figure 5A, bottom panel, lanes 4–9 and 13–18). However, biotinylated hFcRn was only detected on the basolateral plasma membrane, whether in the presence or absence of bovine IgG (serum; Figure 5A, top panel, lanes 14–15 and 17–18, − serum, and lanes 5–6 and 8–9, + serum). The endogenous apical membrane protein GP135 was detected in the same cell lysates only when biotin was
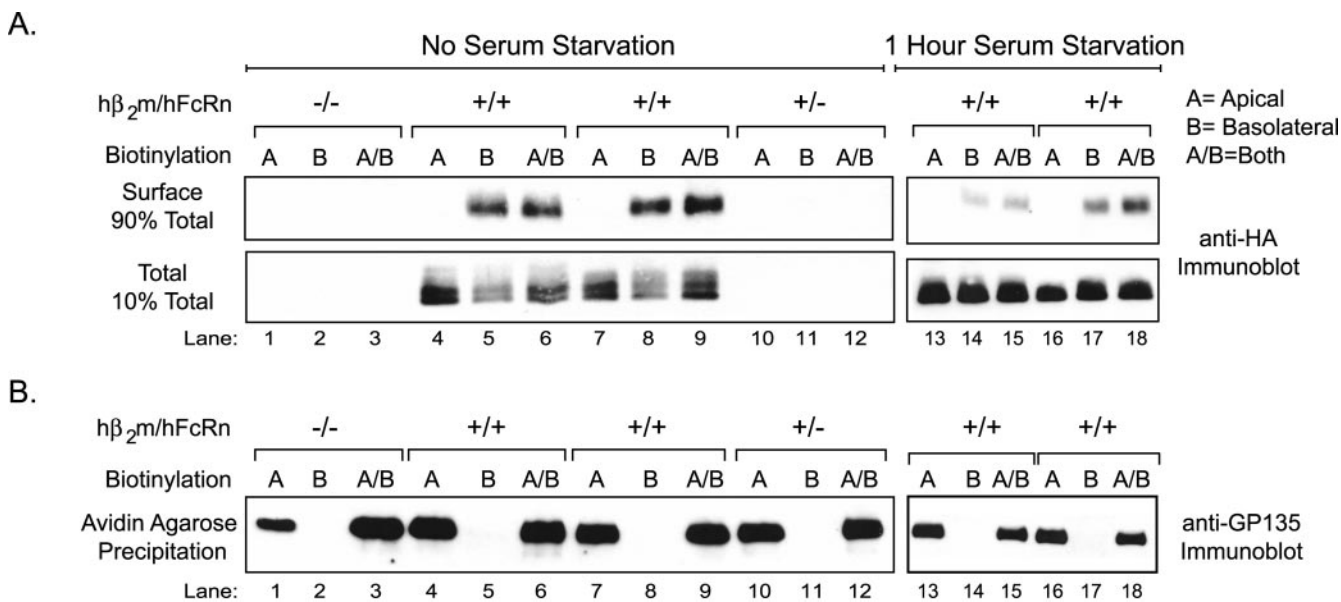
A.

B.

Figure 5. Serum starvation does not stimulate hFcRn redistribution to the apical plasma membrane of MDCK cells. The apical, basolateral, or both membrane domains of confluent MDCK clones were either directly biotinylated (no serum starvation, lanes 1–12), or, alternatively, the cells were first serum starved for 1 h before selective cell surface biotinylation (1 h serum starvation, lanes 13–18). (A) After FcRn immunoprecipitation from 0.5 mg precleared lysate, 10% of the recovered protein was prepared for direct analysis (bottom panel), whereas the remaining 90% was reprecipitated with avidin-agarose (top panel). The samples were analyzed by SDS-PAGE under reducing conditions and FcRn detected by immunoblotting for the N-terminal HA tag. Lysates were derived from a control hFcRn−/hβ$_2$m− MDCK clone, one hFcRn−/hβ$_2$m+ clone, and two hFcRn+/hβ$_2$m+ clones. (B) Remaining surface proteins in the FcRn immunoprecipitation flow-through were precipitated with avidin-agarose. The samples were analyzed by SDS-PAGE under reducing conditions and immunoblotted using the mouse anti-GP135 mAb (n = 3).

applied to apical cell surfaces (Figure 5B), providing evidence for the specificity of cell surface biotin-labeling. Identical results were obtained when monolayers were exposed to human IgG (supplemental Figure 1). Thus at steady state, the cell surface fraction of hFcRn in MDCK cells localizes almost exclusively to the basolateral cell surface, and this is not affected by IgG binding to the receptor. These results differ from those found for the rat receptor (Stefaner *et al.,* 1999; McCarthy *et al.,* 2000; McCarthy *et al.,* 2001; Wu and Simister, 2001).

We next asked if endogenously expressed hFcRn displays a similar polarized cell surface distribution in the T84 and Caco-2 human intestinal epithelial cell lines. Selective cell surface biotinylation was performed with (Figure 6C) or without serum starvation (Figure 6A), and total FcRn was immunoprecipitated from cell lysates with a polyclonal rabbit antiserum specific for the human FcRn cytoplasmic tail. The fraction of immunoprecipitated FcRn containing biotin was analyzed by SDS-PAGE and ligand blot using HRP-labeled neutravidin (neutravidin-HRP). Biotinylated proteins, consistent in size with that predicted for hFcRn and hβ$_2$m were detected by neutravidin-HRP ligand blot in basolaterally biotinylated samples only (Figure 6C, lanes 3, 5, 9, and 11). Exposure to bovine IgG had no effect on the cell surface polarity of hFcRn (Figure 6A, lanes 4, 6, 10, and 12). The nitrocellulose membranes were then stripped and reprobed for hFcRn and hβ$_2$m by immunoblot to demonstrate the presence of hFcRn and hβ$_2$m in all cell lysates (Figure 6, B and D). Further evidence for the specificity of domain-specific biotin-labeling is provided by the same studies on a resident GPI-anchored apical membrane protein, CD55 (Brown *et al.,* 1989). CD55 was detected by immunoblot after avidin-agarose precipitation from lysates of cells that were apically but not basolaterally biotinylated (Figure 6F). Sim-

ilar results were obtained for the resident basolateral membrane protein E-cadherin, which was detected only after basolateral membrane biotinylation (Figure 6E). Thus, the cell surface expression of native hFcRn in the human intestinal cell lines T84 and Caco-2 displays strong basolateral polarity, consistent with our results in MDCK cells.

Human FcRn Moves Transiently though the Apical Membrane

Because hFcRn mediates bidirectional transport across epithelial monolayers, we tested if hFcRn may move transiently to the apical membrane. A mouse mAb against the HA-tag on the N-terminal ectodomain of FcRn was applied to apical or basolateral reservoirs of MDCK cells expressing hFcRn buffered at pH 7.3. The Fc-fragment of mouse IgG2b, the isotype of the anti-HA mAb, does not bind human FcRn appreciably (Ober *et al.,* 2001). After 90-min incubations at the indicated temperatures, the cells were lysed and the mouse anti-HA antibody-antigen complex was precipitated with protein A-Sepharose. At 4°C, hFcRn is immunoprecipitated by mouse anti-HA only when the anti-HA mAb is added to basolateral reservoirs (Figure 7A, bottom panel, lanes 1–2), consistent with our results that at steady state, hFcRn is expressed in detectable quantities on the basolateral but not apical cell surface. When the anti-HA mAb was incubated with MDCK cells at 37°C (bottom panel, lanes 3–4), however, the anti-HA mAb immunoprecipitated hFcRn from both cell surfaces. Given that very little human IgG is internalized from the apical membrane at neutral pH (Figure 3) and that the anti-HA mAb is a significantly weaker ligand for hFcRn than human IgG (Ober *et al.,* 2001), these results suggest that hFcRn moves transiently to the apical membrane where it can bind the anti-HA mAb in the
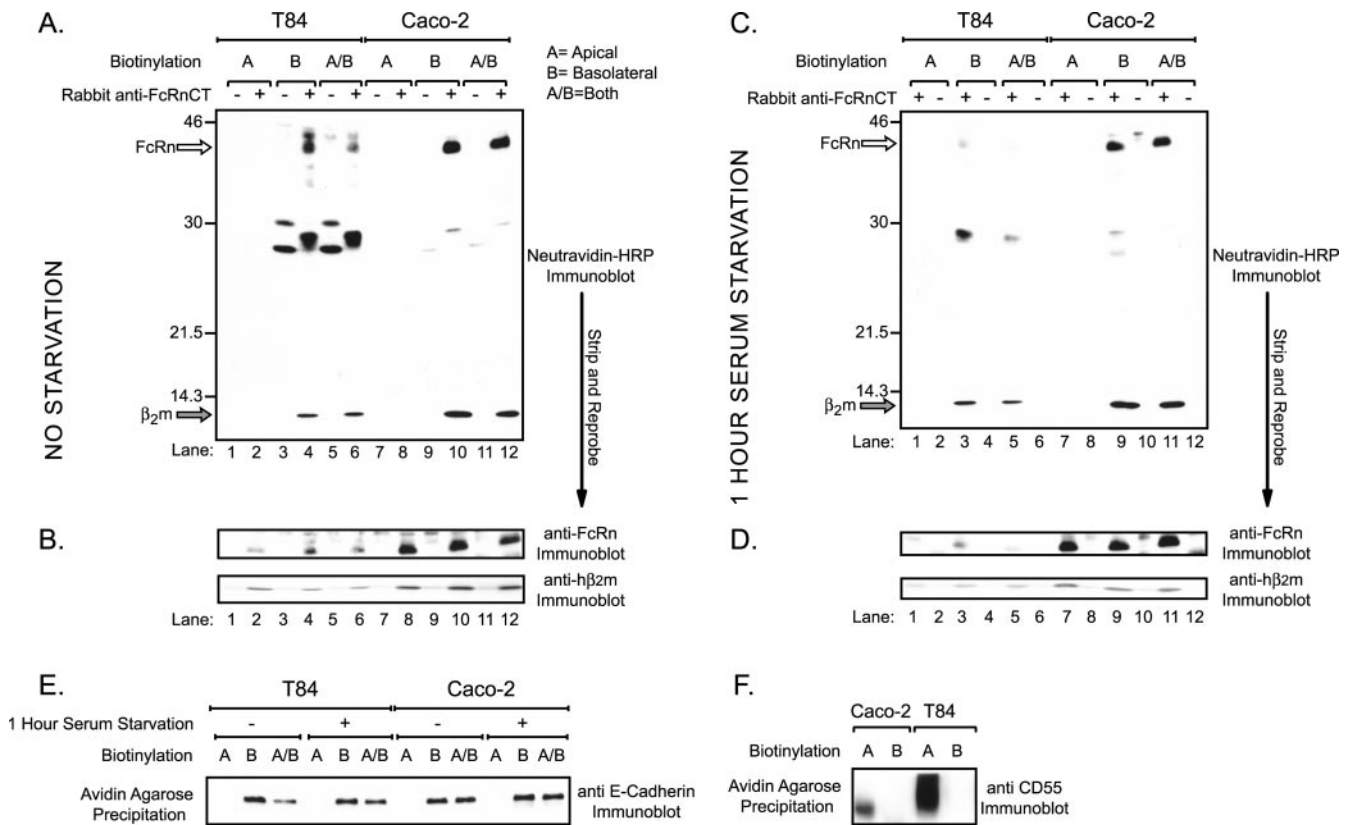
Figure 6. Human FcRn endogenously expressed in the polarized intestinal epithelial cell lines, T84 and Caco-2, is only detected on the basolateral plasma membrane. T84 and Caco-2 cells were grown on Transwell filters until confluent. (A and B) Selective cell surface biotinylation was performed as described in Figure 5 in the absence of prior serum starvation. (C and D) Selective cell surface biotinylation was performed after a 1-h serum starvation. (A and C) FcRn was immunoprecipitated from 1 mg precleared lysates. The precleared material (−) and immunoprecipitates (+) were analyzed by SDS-PAGE under reducing conditions and immunoblotted with neutravidin-HRP. The location of bands consistent with the predicted sizes of hFcRn (open arrow) and $h\beta_2m$ (gray arrow) are indicated on the left of each gel. (B and D) The membranes from A and C, respectively, were stripped and reprobed for hFcRn (top) and $h\beta_2m$ (bottom) as previously described. (E) Surface proteins from 0.1 mg of each lysate were captured by the addition of avidin-agarose. The precipitated surface proteins were analyzed by SDS-PAGE under reducing conditions and immunoblotted with anti–E-cadherin mAb. (F) Surface proteins from 1 mg of lysates following selective cell surface biotinylation were captured by avidin-agarose. The precipitated surface proteins were analyzed by SDS-PAGE under reducing conditions and immunoblotted using a rabbit anti-human CD55 antiserum (n = 3).

apical reservoir. Similar results were obtained when MDCK cells were incubated at 18°C to slow membrane dynamics (bottom panel, lanes 5–6). Immunoblots for β-actin show that equal amounts of total cell lysates were analyzed (Figure 7B). To provide control for cell polarity, antibody capture by the apical membrane protein GP135 was also analyzed. In these experiments, protein A-Sepharose isolated the apically restricted GP135 antigen only after addition of the anti-GP135 mAb to apical reservoirs (Figure 7A, top panel, lanes 3 and 4). These results, together with our observations that low pH at the apical surface increases IgG uptake and transcytosis by hFcRn (Figures 2 and 3), suggest that hFcRn moves transiently to the apical cell surface where it can bind IgG.

Human FcRn Redistributes to the Apical Membrane after Incubation at 18°C and upon Deletion of the Cytoplasmic Tail

Because incubation at 18°C has been demonstrated to block certain membrane trafficking events, including egress of nascent proteins from the *trans*-Golgi network (Matlin and Simons, 1983) and exit of circulating proteins from early and recycling endosomes (Galloway *et al.*, 1983; Dunn *et al.*,

1989), we tested whether low-temperature incubations might affect the strict basolateral cell surface distribution of hFcRn (Figure 8). Filter-grown MDCK cells expressing hFcRn were incubated at 18°C for the indicated times before selective cell surface biotinylation. After 45 min at 18°C, hFcRn was detected on the apical plasma membrane (Figure 8A, top panel, lane 4). The amount of hFcRn located on the apical membrane increased with longer incubation times at 18°C (Figure 8A, top panel, lanes 6–11, and quantified in 8B). The redistribution of hFcRn to apical membranes after low-temperature incubations was not dependent on protein synthesis as assessed using cycloheximide (Figure 8C, and quantified in 8E). Additionally, we examined the effect of lowered temperature on the cell surface distribution of the basolateral membrane trafficking receptor for transferrin (TfnR). Like hFcRn, incubations at 18°C also redistributed TfnR to the apical membrane (Figure 8D, and quantified in 8E). This observation is consistent with previously published results (Gibson *et al.*, 1998) that detailed a temperature-induced redistribution of TfnR in the endosomal system and shows that TfnR moves from the basolateral membrane all the way to the apical membrane under such conditions. In contrast to hFcRn and TfnR, however, the cell
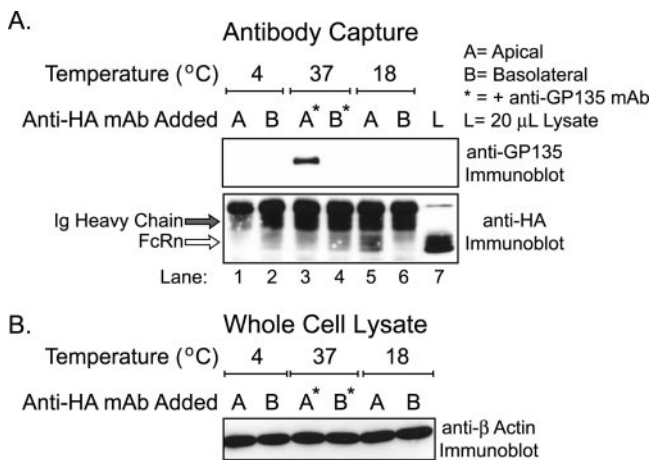
Figure 7. Evidence for a dynamic pool of hFcRn on the apical plasma membrane. Anti-HA mAb, with or without mouse anti-GP135 mAb, was added to the apical or basolateral chamber of confluent monolayers buffered at pH 7.3. After incubation for 90 min at the indicated temperature and subsequent extensive washing, antigen-antibody complexes were captured from equal volumes of lysate with protein A-Sepharose. (A) The recovered samples were analyzed by anti-GP135 (top panel) and anti-HA (bottom panel) immunoblotting as described in Figure 5. (B) A 20-μL aliquot of each lysate, sampled just before washing the protein A-Sepharose precipitates, was analyzed for total protein content by anti–β-actin immunoblotting as described in Figure 1. These data were confirmed utilizing two different hFcRn+/hβ$_2$m+ MDCK clones. Data are presented from a single clone (n = 3).

surface distribution of the resident basolateral membrane protein E-cadherin is not affected by incubation at 18°C (Figure 8F). Thus, the trafficking receptors hFcRn and TnfR redistribute to the apical membrane upon incubation at 18°C. These data imply the presence of a temperature-sensitive step in the normal itinerary of hFcRn and TfnR trafficking that affects the strong basolateral polarity of these proteins at steady state.

Because the cytoplasmic tail of many proteins, including FcRn (Stefaner *et al.,* 1999; McCarthy *et al.,* 2001; Wu and Simister, 2001) and TfnR (Odorizzi *et al.,* 1996; Odorizzi and Trowbridge, 1997), contains basolateral targeting motifs, we tested whether removal of the hFcRn cytoplasmic tail would alter its cell surface distribution. Two independently derived stable MDCK cell clones expressing a tailless hFcRn (hFcRntl−) and hβ$_2$m were prepared and examined for cell surface distribution as described above. In contrast to wild-type hFcRn, the hFcRntl− was detected on both the apical and basolateral membrane domains in roughly equal quantities (Figure 9A). That the strict apical distribution of GP135 was maintained in these clones indicated specificity for cell surface labeling and that all of the MDCK clones analyzed maintained both polarity and junctional integrity throughout the experimental protocol (Figure 9B). Thus, the cytoplasmic tail of hFcRn contains one or more sorting motif(s) that when removed permits redistribution of a large amount of hFcRn (50% of the fraction on the cell surface) from an almost exclusively basolateral cell membrane localization to the apical membrane.

Cell Surface Polarity of hFcRn Does Not Depend on Differential Rates of Endocytosis from Apical or Basolateral Membranes

The strong basolateral cell surface polarity of hFcRn may result from different rates of endocytosis from apical and

basolateral membranes. To test this idea, we examined the rates of hFcRn endocytosis from both cell surfaces. In these studies, we used disulfide-linked biotin (sulfo-NHS-SS-biotin) to label apical or basolateral cell surface proteins at 4°C and then shifted the temperature to 18 or 37°C to allow for endocytosis. Using a membrane-impermeant reducing agent, the biotin tag is removed from only those proteins at the cell surface, whereas biotinylated proteins inside the cell remain labeled with biotin. Thus in these studies, the hFcRn-SS-biotin that is detected by immunoblot after avidin-agarose precipitation represents the fraction of hFcRn that was internalized by endocytosis. As control, the rates of hFcRn endocytosis were compared with that of TfnR using the same method.

The time course of hFcRn endocytosis from the basolateral membrane (Figure 10, A–C) was rapid and similar to that of TfnR at both 18 and 37°C (compare top and bottom panels). Endocytosis of both proteins was slower at 18°C. Immunoblots for β-actin show that equal amounts of total cell lysates were present in each sample during affinity precipitation (Figure 10B). These data are quantified in Figure 10C.

To measure endocytosis of hFcRn and TnfR from the apical membrane, MDCK cell monolayers expressing hFcRn were first incubated overnight at 18°C to redistribute both receptors from the basolateral membrane to the apical membrane. The rates of apical hFcRn and TnfR endocytosis at 37 and 18°C were measured as described above (Figure 10, D–F). As for basolateral hFcRn, the time course of apical hFcRn endocytosis was rapid and similar to that of TfnR at both temperatures (Figure 10D, middle and bottom panels). Endocytosis of the resident apical membrane protein GP135, which is anchored to the cytoskeleton, was not apparent at either temperature (Figure 10D, top panel). Again, immunoblots for β-actin show that equal amounts of total cell lysates were used in each condition (Figure 10E). Figure 10F quantifies these data. These data show that endocytosis of hFcRn from the apical and basolateral membranes occurs at the same rate and with similar efficiency to that of TfnR, consistent with endocytosis of FcRn by clathrin-mediated mechanisms (Rodewald and Kraehenbuhl, 1984). Thus, the redistribution of hFcRn to apical membranes seen during incubations at 18°C or after removal of the hFcRn cytoplasmic tail parallels that of TfnR and cannot be explained by differential rates of endocytosis. These results suggest that the cytoplasmic tail of hFcRn contains a dominant basolateral sorting motif(s) that distributes the receptor basolaterally at steady state.

DISCUSSION

The results of these studies indicate that the fraction of human FcRn on the cell surface of epithelial cells lining mucosal surfaces is strictly polarized to the basolateral membrane. This is explained by the presence of a dominant basolateral sorting motif located in the cytoplasmic tail of the human receptor. Such a strict basolateral polarity of the human FcRn is observed for hFcRn heterologously expressed in canine MDCK cells and endogenously expressed in human intestinal T84 and Caco-2 cell lines. In contrast, the rat FcRn expressed in rat inner medullary collecting duct (IMCD) cells is only weakly polarized to the basolateral plasma membrane (McCarthy *et al.,* 2001; Wu and Simister, 2001), and the opposite polarity is observed for the low-affinity Fc receptor FcγRIIb fused to the rat FcRn cytoplasmic tail in MDCK cells (Stefaner *et al.,* 1999). We also believe that the studies on FcRn in rat IMCD cells (McCarthy *et al.,* 2000, 2001; McCarthy *et al.,* 2001) are not conclusive as a significant fraction of the rat FcRn found on the cell surface
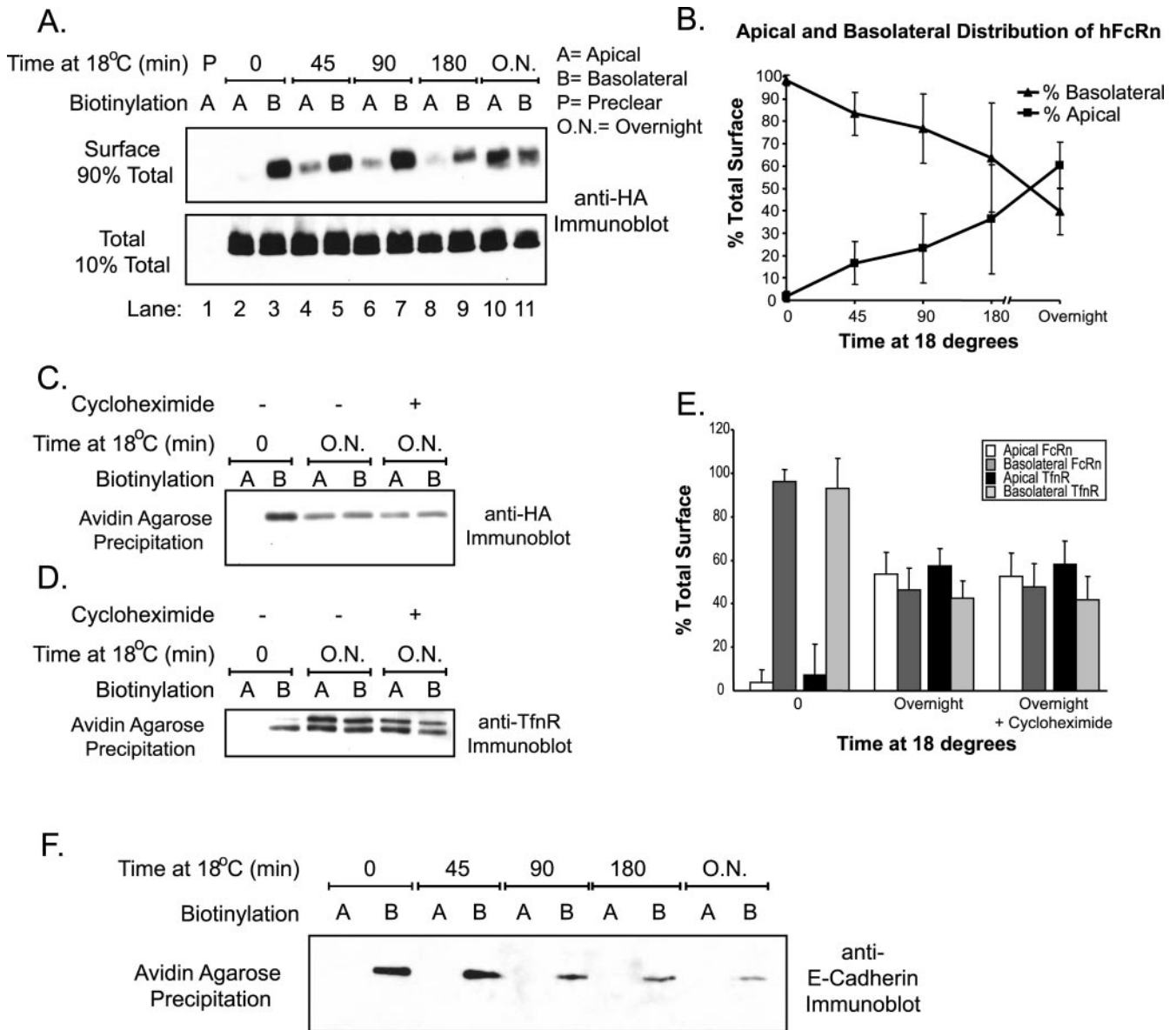
Figure 8. Loss of strict hFcRn basolateral polarity upon prolonged incubation at 18°C. Confluent MDCK monolayers were incubated at 18°C for the indicated times before selective cell surface biotinylation. (A) FcRn immunoprecipitation, avidin-agarose reprecipitation, and anti-HA immunoblotting were performed as described in Figure 5. (B) Data from three separate experiments with two individual hFcRn+/hβ_2m+ MDCK clones were quantitated using Quantitation One software (Bio-Rad). After normalization to the amount of hFcRn present in each immunoprecipitate, the relative apical and basolateral distribution of hFcRn was calculated as percentages of the total surface hFcRn for each timepoint as follows: $A/(A+B) \times 100$ and $B/(A+B) \times 100$, where A is the normalized volume of hFcRn detected on the apical surface and B is the normalized volume of hFcRn on the basolateral membrane. (C and D) Where indicated, 10 μM cycloheximide was added to the medium during the overnight incubation at 18°C. Surface proteins were captured by the addition of avidin-agarose and FcRn (C) or TfnR (D) detected by immunoblot as described in Figure 5. (E) Data from three separate experiments and two different hFcRn+/hβ_2m+ MDCK clones were quantitated as in B. After β-actin normalization, the relative apical and basolateral distribution of hFcRn and TfnR on the apical or basolateral cell surface at 37, 18, and 18°C in the presence of cycloheximide was calculated as in B. (F) Avidin-agarose precipitation of the anti-FcRn flow-through from (A) and anti–E-cadherin immunoblotting were performed as previously described (n = 3).

contains the ER form of N-linked oligosaccharides, suggesting the presence of nonphysiologic trafficking in this model system.

The different cell surface polarities displayed by the full-length rat and human receptor correlates with different cellular physiology. Here, we find that the hFcRn transports IgG more efficiently in the basolateral to apical direction. This is opposite to that found for the rat receptor (McCarthy *et al.,* 2000), but consistent with our previous work (Claypool

et al., 2002) and with the function of hFcRn in placental endothelial cells (Antohe *et al.,* 2001). The reason for these differences in trafficking of the human and rat receptor are not known, though perhaps they are related to a stronger apical membrane-targeting motif located somewhere in the structure of the rat receptor. A candidate apical-sorting motif might be the four N-linked glycosylation sites present in the ectodomain of the rat FcRn, three of which are lacking in the human receptor.
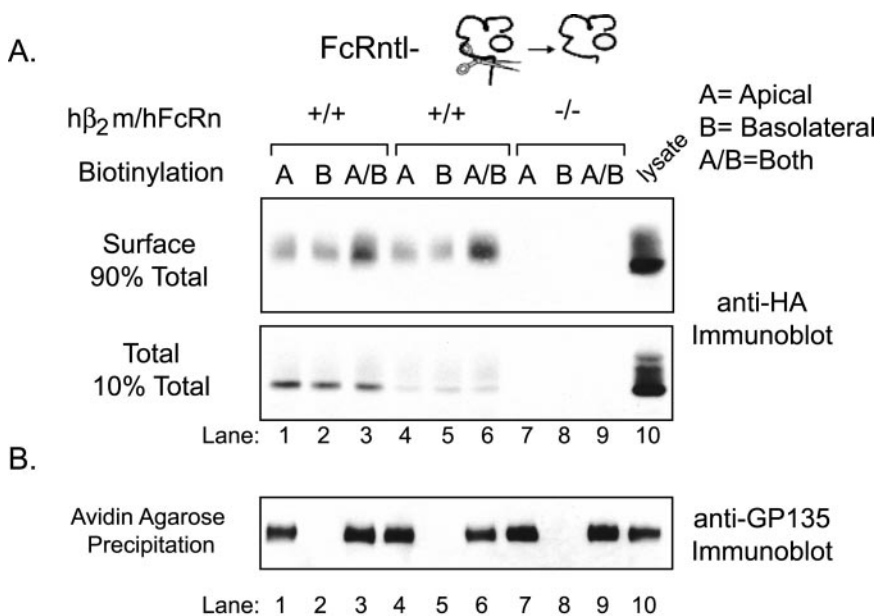
A.

B.

Figure 9. Tailless hFcRn is detected on both the apical and basolateral plasma membrane domains. Selective cell surface biotinylation of confluent MDCK monolayers was performed as described in Figure 5. (A) FcRn immunoprecipitation, detection of membrane-associated hFcRn, and FcRn immunoblotting were performed as described in Figure 5. Lysates were derived from a control hFcRn−/hβ_2m− MDCK clone and two clones coexpressing hFcRntl− and hβ_2m (hFcRn+/hβ_2m+). Ten micrograms of whole cell lysate was analyzed directly to confirm the presence and migration of tailless hFcRn after immunoprecipitation (lane 10). (B) Avidin-agarose precipitation of the anti-FcRn flow-through and anti-GP135 immunoblotting were performed as described in Figure 5 (n = 3).

Our studies show that human FcRn has a strong basolateral targeting motif located in the cytoplasmic tail, as removal of the cytoplasmic tail by mutagenesis redistributes the receptor apically. This cannot be explained by differential rates of endocytosis from apical and basolateral membrane domains. Thus, the strong cell surface polarity displayed by FcRn results from dominant basolateral sorting. At least one step in the sorting of hFcRn to basolateral membranes, however, must be differentially sensitive to low temperature because incubations at 18°C redistributes the wild-type receptor apically. Redistribution of hFcRn still occurs in the absence of protein synthesis, indicating that dominant basolateral sorting for hFcRn occurs in the endosome rather than in the secretory pathway.

Very similar results were observed with the membrane trafficking receptor for transferrin. The cytoplasmic tail of TnfR also contains a strong basolateral targeting motif, and the receptor is strictly localized to the basolateral membrane at steady state (Odorizzi *et al.*, 1996; Odorizzi and Trowbridge, 1997). Like hFcRn, a small fraction of the TfnR can move bidirectionally across polarized MDCK cell monolayers by sorting through a common endosomal compartment (Odorizzi *et al.*, 1996). Thus, the strong basolateral polarity of a protein at steady state does not preclude the possibility of bidirectional transcytosis. It is possible that the cytoplasmic tails of TfnR and hFcRn share a functionally similar structure. In contrast to TfnR, however, FcRn localizes predominantly to an apical intracellular compartment, which may represent the common endosome. Also trafficking by FcRn through the transcytotic pathway cannot be the same as for TfnR because it is more efficient, delivering physiological levels of IgG across the monolayer in both directions (Spiekermann *et al.*, 2002 and our unpublished results).

Interestingly, TfnR, like hFcRn, was demonstrated to undergo a temperature-induced redistribution to the apical cell surface. Another basolateral membrane protein, E-cadherin, maintained its strict basolateral polarity even after an overnight incubation at 18°C, demonstrating that the observed 18°C effect is not common to all basolaterally restricted receptors. Thus, the cytoplasmic tails of TfnR and hFcRn share a functionally similar motif that is active in the endosomal system as a basolateral cell surface retrieval signal

and that is temperature sensitive. Mutagenesis studies had previously determined that the cytoplasmic tail of TfnR contained separate basolateral sorting motifs that were functional either in the biosynthetic or endocytic pathways (Odorizzi and Trowbridge, 1997). Moreover, residues 29–35 of the cytoplasmic tail were identified as the motif operative in the biosynthetic pathway. In contrast, the molecular nature of the endocytic basolateral motif eluded identification. Similarly, although previous work on rat FcRn revealed the presence of a basolateral sorting signal in the cytoplasmic tail of rat FcRn (Stefaner *et al.*, 1999; Wu and Simister, 2001), this motif has not been identified, although a di-leucine motif in the cytoplasmic tail has been clearly demonstrated to not encode basolateral sorting information. Perhaps, the observed redistribution of both TfnR and hFcRn at 18°C will provide a useful assay that combined with site-directed mutagenesis will identify these elusive endocytically active, basolateral determinants.

Even with the strict basolateral membrane polarity of FcRn at steady state, we find that hFcRn moves transiently to the apical plasma membrane. This is evidenced most clearly by the increase in internalization and transcytosis of IgG when apical reservoirs are clamped at pH 6.0, which is permissive for FcRn binding, and by capture of an apically applied antibody at 37 but not 4°C. The rapid and transient appearance of hFcRn at the apical cell surface may reflect an adaptation to protect hFcRn from digestive enzymes present in luminal secretions. In support of this view, it was previously demonstrated that pretreatment of neonatal rat proximal small intestinal loops with luminal trypsin drastically reduced the quantity of pH-dependent IgG binding to apical membranes (Borthistle *et al.*, 1977).

The immediate luminal environment adjacent to the apical membrane of cells lining the intestine and probably all other Na$^+$-absorbing mucosal surfaces in the human and other mammals is acidic because of the activity of the sodium-hydrogen exchanger NHE3 (Tse *et al.*, 1993; Noel *et al.*, 1996). The NHE3 creates an inwardly directed proton gradient across the brush border membrane of intestinal epithelial cells that is harnessed by proton-coupled solute-transporters to drive peptide and Fe^{2+} absorption (Liang *et al.*, 1995; Gunshin *et al.*, 1997). Because FcRn releases IgG only very
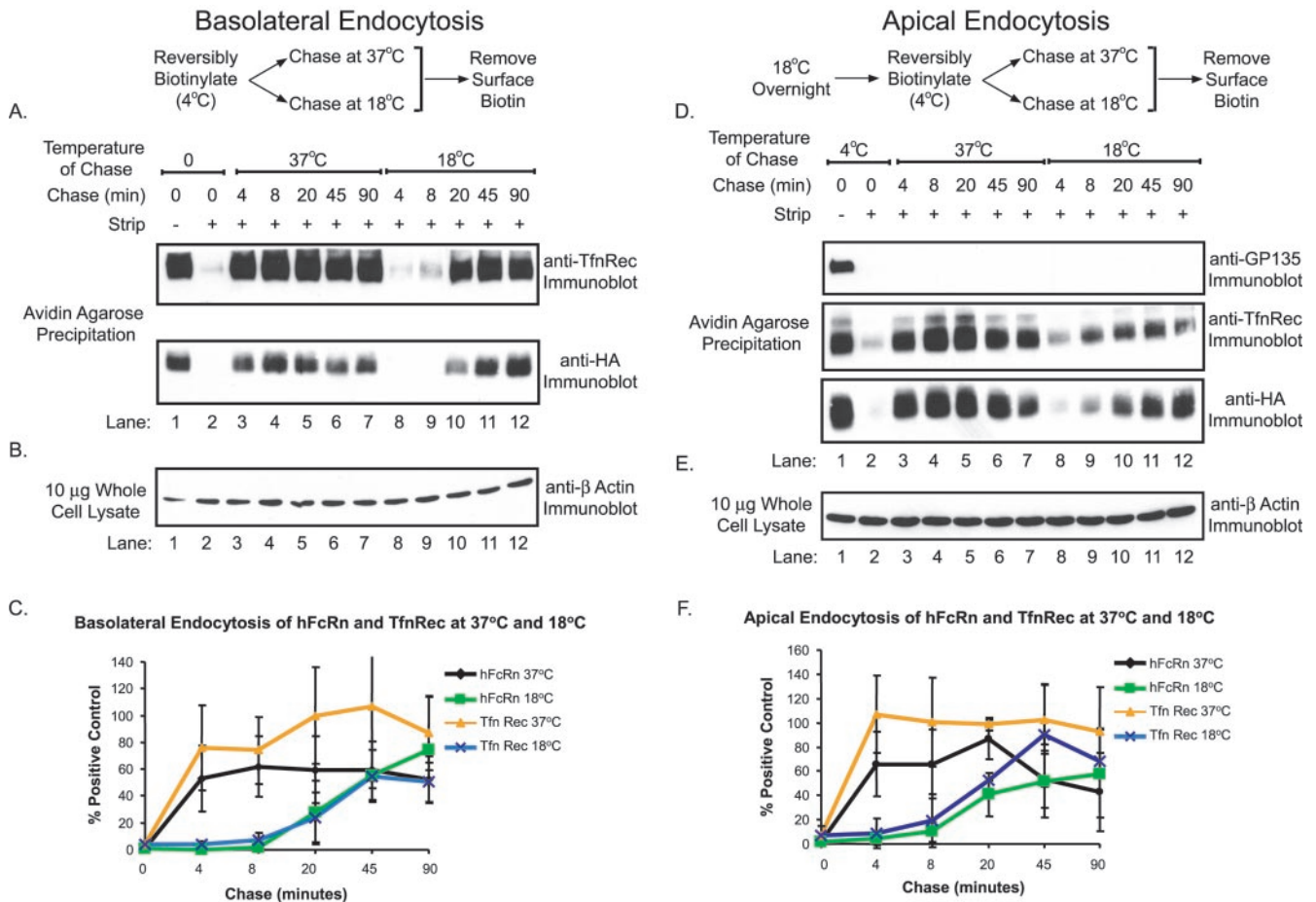
Figure 10. Endocytosis of hFcRn from the apical and basolateral plasma membranes is delayed at low temperature. (A–C) Confluent MDCK monolayers were biotinylated on the basolateral plasma membrane with the cleavable biotin analog, sulfo-NHS-SS-biotin. (D–F) To accumulate hFcRn on the apical surface, an overnight 18°C incubation was performed before biotinylation. (A and D) After quenching of unreacted biotin, filters were incubated for the indicated times at 37 or 18°C and then rapidly cooled to 4°C. Remaining membrane-associated biotin was then removed from the apical and basolateral membranes with a glutathione-based reducing solution (lanes 3–12). Two filters per experiment were maintained at 4°C throughout the experiment, serving as a biotinylation control (lane 1) and a control for the efficiency of biotin reduction (lane 2). Total biotinylated surface proteins were precipitated with avidin-agarose and analyzed by immunoblot. (B and E) β-actin immunoblot of each lysate (10 μg) was performed as previously described. (C and F) Data from two different hFcRn$+$/hβ_2m$+$ MDCK clones were quantitated as in Figure 8. After normalization to β-actin, the relative amounts of hFcRn and TfnR endocytosed at 37 and 18°C at each time point were expressed as a percentage of the total initial cell surface receptor (n = 2).

slowly at acidic pH, we propose that in vivo the FcRn-IgG complex may remain intact after transport to the apical membrane. Here, the FcRn-IgG complex may bind cognate luminal antigens and then efficiently recycle back into and across the epithelial barrier where the immune complex is released for processing by dendritic cells located in the subepithelial space. In this way, FcRn and IgG may participate in immune surveillance at mucosal surfaces.

Finally, our results show that even though hFcRn in MDCK cells mediates the bidirectional transport of IgG across the monolayer, hFcRn does not appear to redistribute from its predominant intracellular or basolateral cell surface distribution after ligand binding. The lack of any marked redistribution of hFcRn at the cell surface or within vesicles induced by bovine IgG was perhaps not unexpected given the low affinity of hFcRn for bovine IgG (Ober *et al.,* 2001) and the recent retraction of studies claiming otherwise (Retraction, 2002; Ramalingam *et al.,* 2002). Although the lack of effect on hFcRn distribution after receptor binding to human IgG is somewhat counterintuitive, as the receptor presum-

ably moves with its ligand into and across the cell, is consistent with the fact that the FcγRII/rat FcRn chimera was demonstrated capable of bidirectional transport in the absence of ligand (Stefaner *et al.,* 1999). Thus, it may be argued that IgG binding is not a strict requirement for FcRn transcytosis. Further, it is possible that the bidirectional trafficking of hFcRn, and thus transport of IgG, is constitutive with no regulation by bound cargo. Directional transport might therefore be specified by the presence of gradients external to FcRn, such as ligand and pH gradients. That these types of gradients are capable of powerfully harnessing this receptor system is perhaps best exemplified in the classical setting for FcRn; the neonatal rat intestine.

ACKNOWLEDGMENTS

REFERENCES

Retraction. (2002). EMBO J. *21*, 5953.

Abrahamson, D.R., and Rodewald, R. (1981). Evidence for the sorting of endocytic vesicle contents during the receptor-mediated transport of IgG across the newborn rat intestine. J. Cell Biol. *91*, 270–280.

Antohe, F., Radulescu, L., Gafencu, A., Ghetie, V., and Simionescu, M. (2001). Expression of functionally active FcRn and the differentiated bidirectional transport of IgG in human placental endothelial cells. Hum. Immunol. *62*, 93–105.

Berryman, M., and Rodewald, R. (1995). Beta 2-microglobulin co-distributes with the heavy chain of the intestinal IgG-Fc receptor throughout the trans-epithelial transport pathway of the neonatal rat. J. Cell Sci. *108*, 2347–2360.

Borthistle, B.K., Kubo, R.T., Brown, W.R., and Grey, H.M. (1977). Studies on receptors for IgG on epithelial cells of the rat intestine. J. Immunol. *119*, 471–476.

Borvak, J., Richardson, J., Medesan, C., Antohe, F., Radu, C., Simionescu, M., Ghetie, V., and Ward, E.S. (1998). Functional expression of the MHC class I-related receptor, FcRn, in endothelial cells of mice. Int. Immunol. *10*, 1289–1298.

Brambell, F.W. (1966). The transmission of immunity from mother to young and the catabolism of immunoglobulins. Lancet *2*, 1087–1093.

Brown, D.A., Crise, B., and Rose, J.K. (1989). Mechanism of membrane anchoring affects polarized expression of two proteins in MDCK cells. Science *245*, 1499–1501.

Brown, P.S., Wang, E., Aroeti, B., Chapin, S.J., Mostov, K.E., and Dunn, K.W. (2000). Definition of distinct compartments in polarized Madin-Darby canine kidney (MDCK) cells for membrane-volume sorting, polarized sorting and apical recycling. Traffic *1*, 124–140.

Burmeister, W.P., Huber, A.H., and Bjorkman, P.J. (1994). Crystal structure of the complex of rat neonatal Fc receptor with Fc [see comments]. Nature *372*, 379–383.

Casanova, J.E., Apodaca, G., and Mostov, K.E. (1991). An autonomous signal for basolateral sorting in the cytoplasmic domain of the polymeric immuno-globulin receptor. Cell *66*, 65–75.

Cepek, K.L., Shaw, S.K., Parker, C.M., Russell, G.J., Morrow, J.S., Rimm, D.L., and Brenner, M.B. (1994). Adhesion between epithelial cells and T lympho-cytes mediated by E-cadherin and the alpha E beta 7 integrin. Nature *372*, 190–193.

Claypool, S.M., Dickinson, B.L., Yoshida, M., Lencer, W.I., and Blumberg, R.S. (2002). Functional reconstitution of human FcRn in Madin-Darby canine kidney cells requires co-expressed human beta 2-microglobulin. J. Biol. Chem. *277*, 28038–28050.

Dickinson, B.L., Badizadegan, K., Wu, Z., Ahouse, J.C., Zhu, X., Simister, N.E., Blumberg, R.S., and Lencer, W.I. (1999). Bidirectional FcRn-dependent IgG transport in a polarized human intestinal epithelial cell line. J. Clin. Invest. *104*, 903–911.

Dunn, K., McGraw, T., and Maxfield, F. (1989). Iterative fractionation of recycling receptors from lysosomally destined ligands in an early sorting endosome. J. Cell Biol. *109*, 3303–3314.

Firan, M., Bawdon, R., Radu, C., Ober, R.J., Eaken, D., Antohe, F., Ghetie, V., and Ward, E.S. (2001). The MHC class I-related receptor, FcRn, plays an essential role in the maternofetal transfer of gamma-globulin in humans. Int. Immunol. *13*, 993–1002.

Galloway, C.J., Dean, G.E., Marsh, M., Rudnick, G., and Mellman, I. (1983). Acidification of macrophage and fibroblast endocytic vesicles in vitro. Proc. Natl. Acad. Sci. USA *80*, 3334–3338.

Gibson, A. *et al.* (1998). Sorting mechanisms regulating membrane protein traffic in the apical transcytotic pathway of polarized MDCK cells. J. Cell Biol. *143*, 81–94.

Graeve, L., Drickamer, K., and Rodriguez-Boulan, E. (1989). Polarized endo-cytosis by Madin-Darby canine kidney cells transfected with functional chicken liver glycoprotein receptor. J. Cell Biol. *109*, 2809–2816.

Gunshin, H., Mackenzie, B., Berger, U.V., Gunshin, Y., Romero, M.F., Boron, W.F., Nussberger, S., Gollan, J.L., and Hediger, M.A. (1997). Cloning and characterization of a mammalian proton-coupled metal-ion transporter. Nature *388*, 482–488.

Johansen, F.E., Natvig Norderhaug, I., Roe, M., Sandlie, I., and Brandtzaeg, P. (1999). Recombinant expression of polymeric IgA: incorporation of J chain and secretory component of human origin. Eur. J. Immunol. *29*, 1701–1708.

Jones, E., and Waldmann, T. (1972). The mechanism of intestinal uptake and transcellular transport of IgG in neonatal rat. J. Clin. Invest. *51*, 2916–2927.

Kim, J.K., Tsen, M.F., Ghetie, V., and Ward, E.S. (1994). Localization of the site of the murine IgG1 molecule that is involved in binding to the murine intestinal Fc receptor. Eur. J. Immunol. *24*, 2429–2434.

Kobayashi, N., Suzuki, Y., Tsuge, T., Okumura, K., Ra, C., and Tomino, Y. (2002). FcRn-mediated transcytosis of immunoglobulin G in human renal proximal tubular epithelial cells. Am. J. Physiol. Renal Physiol. *282*, F358–F365.

Leung, S.M., Rojas, R., Maples, C., Flynn, C., Ruiz, W.G., Jou, T.S., and Apodaca, G. (1999). Modulation of endocytic traffic in polarized Madin-Darby canine kidney cells by the small GTPase RhoA. Mol. Biol. Cell *10*, 4369–4384.

Liang, R., Fei, Y.J., Prasad, P.D., Ramamoorthy, S., Han, H., Yang-Feng, T.L., Hediger, M.A., Ganapathy, V., and Leibach, F.H. (1995). Human intestinal H+/peptide cotransporter. Cloning, functional expression, and chromosomal localization. J. Biol. Chem. *270*, 6456–6463.

Matlin, K.S., and Simons, K. (1983). Reduced temperature prevents transfer of a membrane glycoprotein to the cell surface but does not prevent terminal glycosylation. Cell *34*, 233–243.

McCarthy, K.M., Lam, M., Subramanian, L., Shakya, R., Wu, Z., Newton, E.E., and Simister, N.E. (2001). Effects of mutations in potential phosphorylation sites on transcytosis of FcRn. J. Cell Sci. *114*, 1591–1598.

McCarthy, K.M., Yoong, Y., and Simister, N.E. (2000). Bidirectional transcy-tosis of IgG by the rat neonatal Fc receptor expressed in a rat kidney cell line: a system to study protein transport across epithelia. J. Cell Sci. *113*, 1277–1285.

Medesan, C., Radu, C., Kim, J.K., Ghetie, V., and Ward, E.S. (1996). Localiza-tion of the site of the IgG molecule that regulates maternofetal transmission in mice. Eur. J. Immunol. *26*, 2533–2536.

Mostov, K.E., and Deitcher, D.L. (1986). Polymeric immunoglobulin receptor expressed in MDCK cells transcytoses IgA. Cell *46*, 613–621.

Noel, J., Roux, D., and Pouyssegur, J. (1996). Differential localization of Na+/H+ exchanger isoforms (NHE1 and NHE3) in polarized epithelial cell lines. J. Cell Sci. *109 (Pt 5)*, 929–939.

Norderhaug, L., Olafsen, T., Michaelsen, T.E., and Sandlie, I. (1997). Versatile vectors for transient and stable expression of recombinant antibody molecules in mammalian cells. J. Immunol. Methods *204*, 77–87.

Ober, R.J., Radu, C.G., Ghetie, V., and Ward, E.S. (2001). Differences in promiscuity for antibody-FcRn interactions across species: implications for therapeutic antibodies. Int. Immunol. *13*, 1551–1559.

Odorizzi, G., Pearse, A., Domingo, D., Trowbridge, I.S., and Hopkins, C.R. (1996). Apical and basolateral endosomes of MDCK cells are interconnected and contain a polarized sorting mechanism. J. Cell Biol. *135*, 139–152.

Odorizzi, G., and Trowbridge, I.S. (1997). Structural requirements for baso-lateral sorting of the human transferrin receptor in the biosynthetic and endocytic pathways of Madin-Darby canine kidney cells. J. Cell Biol. *137*, 1255–1264.

Ojakian, G.K., and Schwimmer, R. (1988). The polarized distribution of an apical cell surface glycoprotein is maintained by interactions with the cy-toskeleton of Madin-Darby canine kidney cells. J. Cell Biol. *107*, 2377–2387.

Praetor, A., Ellinger, I., and Hunziker, W. (1999). Intracellular traffic of the MHC class I-like IgG Fc receptor, FcRn, expressed in epithelial MDCK cells. J. Cell Sci. *112*, 2291–2299.

Ramalingam, T.S., Detmer, S.A., Martin, W.L., and Bjorkman, P.J. (2002). IgG transcytosis and recycling by FcRn expressed in MDCK cells reveals ligand-induced redistribution. EMBO J. *21*, 590–601.

Roberts, D.M., Guenthert, M., and Rodewald, R. (1990). Isolation and charac-terization of the Fc receptor from the fetal yolk sac of the rat. J. Cell Biol. *111*, 1867–1876.

Rodewald, R. (1970). Selective antibody transport in the proximal small intestine of the neonatal rat. J. Cell Biol. *45*, 635–640.

Rodewald, R. (1976). pH-dependent binding of immunoglobulins to intestinal cells of the neonatal rat. J. Cell Biol. *71*, 666–669.

Rodewald, R., and Kraehenbuhl, J.P. (1984). Receptor-mediated transport of IgG. J. Cell Biol. *99*, 159s–164s.

Simister, N.E., and Mostov, K.E. (1989). An Fc receptor structurally related to MHC class I antigens. Nature *337*, 184–187.

Singer, K.L., and Mostov, K.E. (1998). Dimerization of the polymeric immunoglobulin receptor controls its transcytotic trafficking. Mol. Biol. Cell *9*, 901–915.

Spiekermann, G.M., Finn, P.W., Ward, E.S., Dumont, J., Dickinson, B.L., Blumberg, R.S., and Lencer, W.I. (2002). Receptor-mediated immunoglobulin G transport across mucosal barriers in adult life: functional expression of FcRn in the mammalian lung. J. Exp. Med. *196*, 303–310.

Stefaner, I., Praetor, A., and Hunziker, W. (1999). Nonvectorial surface transport, endocytosis via a Di-leucine-based motif, and bidirectional transcytosis of chimera encoding the cytosolic tail of rat FcRn expressed in Madin-Darby canine kidney cells. J. Biol. Chem. *274*, 8998–9005.

Story, C.M., Mikulska, J.E., and Simister, N.E. (1994). A major histocompatibility complex class I-like Fc receptor cloned from human placenta: possible role in transfer of immunoglobulin G from mother to fetus. J. Exp. Med. *180*, 2377–2381.

Tse, C.M., Levine, S.A., Yun, C.H., Brant, S.R., Pouyssegur, J., Montrose, M.H., and Donowitz, M. (1993). Functional characteristics of a cloned epithelial Na+/H+ exchanger (NHE3): resistance to amiloride and inhibition by protein kinase C. Proc. Natl. Acad. Sci. USA *90*, 9110–9114.

Wang, E., Brown, P.S., Aroeti, B., Chapin, S.J., Mostov, K.E., and Dunn, K.W. (2000). Apical and basolateral endocytic pathways of MDCK cells meet in acidic common endosomes distinct from a nearly-neutral apical recycling endosome. Traffic *1*, 480–493.

Ward, E.S., Zhou, J., Ghetie, V., and Ober, R.J. (2003). Evidence to support the cellular mechanism involved in serum IgG homeostasis in humans. Int. Immunol. *15*, 187–195.

Wu, Z., and Simister, N.E. (2001). Tryptophan- and dileucine-based endocytosis signals in the neonatal fc receptor. J. Biol. Chem. *276*, 5240–5247.

Zhu, X. *et al.* (2001). MHC class I-related neonatal Fc receptor for IgG is functionally expressed in monocytes, intestinal macrophages, and dendritic cells. J. Immunol. *166*, 3266–3276.